American Journal of Pathology, Vol. 154, No. 4, April 1999

Morphological, Histochemical, Immunohistochemical, and Ultrastructural Characterization of Tumors and Dysplastic and Non-Neoplastic Lesions Arising in BK Virus/*tat* Transgenic Mice

Giuseppe Altavilla,* Cecilia Trabanelli,† Michela Merlin,† Antonella Caputo,† Massimo Lanfredi,‡ Giuseppe Barbanti-Brodano,† and Alfredo Corallini†

From the Institute of Pathologic Anatomy and Histology, University of Padova, Padova, the Department of Experimental and Diagnostic Medicine,† Section of Microbiology and the Interdepartment Centre for Biotechnology, and the Department of Biology,‡ Evolutionary Biology Branch, University of Ferrara, Ferrara, Italy*

To study the role in AIDS pathogenesis of the human immunodeficiency virus type 1 (HIV-1) Tat protein, a transactivator of viral and cellular genes, we generated transgenic mice with a recombinant DNA containing BK virus (BKV) early region and the HIV-1 *tat* gene, directed by its own promoter-enhancer. DNA hybridization revealed that the transgene is stably maintained in all organs of transgenic mice as a tandem insertion in a number of copies ranging from 5 to 20 per cell. In addition, *tat* and BKV RNA were expressed in all tissues. Transgenic mice developed three types of lesions: 1) tumors, 2) hyperplastic and dysplastic lesions, and 3) non-neoplastic lesions. Tumors of different histotypes, such as lymphomas, adenocarcinomas of skin glands, leiomyosarcomas, skin squamous cell carcinomas, hepatomas, hepatocarcinomas, and cavernous liver hemangiomas, developed in 29% of transgenic animals. The majority of tumors were malignant, invasive, and producing metastases. Conversely, tumors of only two histotypes (lymphomas and adenocarcinomas of skin glands) appeared in control mice. Hyperplastic and dysplastic lesions were more frequent in transgenic than in control mice and involved the skin or its adnexes, the liver and the rectum, indicating multiple targets for the activity of the transgene. Pyelonephritis, frequently complicated with hydronephrosis, inflammatory eye lesions, and amyloid depositions represented the most frequent non-neoplastic lesions detected in transgenic mice. Many of the pathological findings observed in this animal model are comparable to similar lesions appearing in AIDS patients, suggesting a relevant role for Tat in the pathogenesis of such lesions during the course of AIDS. *(Am J Pathol 1999, 154:1231–1244)*

Several types of tumors are associated to human immunodeficiency virus type 1 (HIV-1) infection and AIDS.[1–3] Epidemiological investigations established that non-Hodgkin's B-cell lymphoma (NHL) and Kaposi's sarcoma (KS) significantly increase in HIV-1-infected patients.[4–6] Moreover, other tumors, such as basal cell and squamous cell skin carcinoma, malignant melanoma, and carcinoma of the rectum and of the uterine cervix as well as hepatocellular carcinoma are frequently present as a complication of AIDS.[7] The lack of immune surveillance that causes a state of severe immunodeficiency in HIV-1 infection and AIDS plays a major role in the induction of these tumors. However, reactivation of latent viral infections may participate in AIDS-associated oncogenesis. Indeed, Epstein-Barr virus is frequently reactivated in NHL in AIDS patients,[8] and KS has been associated to some viruses such as cytomegalovirus,[9–12] retroviruses,[13] human papillomavirus,[14,15] BK virus (BKV),[16–18] HHV-6,[19] and HHV-8.[20] Moreover, the Tat protein of HIV-1 is involved in tumor pathogenesis in HIV-1-infected patients. Tat is an early nonstructural protein necessary for virus replication,[21,22] which is released by HIV-1-infected cells[23,24] and is taken up by uninfected cells.[25,26] Tat induces growth, adhesion, migration, and invasion of KS spindle cells[27–29] and is a heparin-binding angiogenic growth factor involved in the development of KS.[23,30] Experimental evidence also indicates that Tat

Supported by funds from "Ministero dell'Università e della Ricerca Scientifica e Tecnologica" (MURST 60%, 1992–1997) to G. Altavilla and to A. Corallini and from the AIDS Project of the Italian Ministry of Health (AIDS Project 1997, Istituto Superiore di Sanità, Rome) to A. Caputo.

Accepted for publication January 22, 1999.

Address reprint requests to Dr. Giuseppe Altavilla, Institute of Pathologic Anatomy and Histology, University of Padova, Via Gabelli 61, I-35100 Padova, Italy. E-mail: altavill@ux1.unipd.it.

regulates the expression of cellular genes, modulating cell functions.[31–33] Tat is highly angiogenic *in vivo*,[30,34] and transgenic mice expressing the *tat* gene develop skin lesions closely resembling the early phases of KS.[35,36]

In a previous study, transgenic mice were generated by means of a recombinant DNA (pRPU3R-Tat) containing BKV early region and the HIV-1 *tat* gene, directed by the HIV-1 long terminal repeat (LTR). BKV early region encodes the viral T antigen (TAg), which is a potent transcriptional activator of HIV-1 LTR, thus inducing expression of Tat in all organs and tissues of transgenic mice. BKV/*tat* transgenic animals developed vascular lesions in the dermis, skin tumors, lymphomas, liver cell dysplasia, and hepatocellular carcinoma.[36] As an extension of our previous findings, in this study we have analyzed in detail the morphological, histochemical, immunohistochemical, and ultrastructural characteristics of tumors, of hyperplastic and dysplastic lesions, and of non-neoplastic lesions arising in BKV/*tat* transgenic mice.

Materials and Methods

Recombinant Plasmid Containing the tat Gene and BKV Early Region

The plasmid used to generate transgenic mice is pRPU3*tat*.[36] This recombinant DNA contains *tat* cDNA directed by its own promoter-enhancer, the HIV-1 LTR. In addition, it contains the complete BKV early region, consisting of the coding sequences for large T antigen and small t antigen as well as the early promoter and enhancer, the replication origin, and poly A sequences. This construct produces three mRNAs, one transcribed from *tat* cDNA and two transcribed from BKV early region, expressing large T antigen and small t antigen, respectively.

Transgenic Mice

The generation of BDF transgenic mice carrying BKV/*tat* sequences has been previously described.[36] Seven founder mice were identified. Each founder gave rise to a heterozygous transgenic mouse line by crossing initially with normal BDF mice and then with heterozygous transgenic mice of the same lineage to obtain animals homozygous for the transgene. Homozygous transgenic mice were later crossed with outbred CD1 mice, a strain particularly sensitive to the effects of *tat*.[35] Control animals were normal BDF mice and BDF crossed with CD1 mice.

Animal Examination

Animals were routinely examined twice a week for the appearance of symptoms, new phenotypes, and tumors. All mice either died of natural causes or were sacrificed for advanced symptoms or lesions and were subjected to autopsy. Organs were taken for histological and histochemical examination and for molecular studies.

Histological, Histochemical, and Immunohistochemical Procedures

Tissue samples taken at autopsy were fixed in 10% formalin in phosphate-buffered saline (PBS) for 12 to 24 hours and embedded in paraffin. A fragment of each sample was also cryopreserved at −80°C. Paraffin-embedded sections (3 to 5 μm) were stained with hematoxylin and eosin (H&E) and treated by periodic acid-Shiff (PAS) reaction. Warthin-Starry silver stain[37] was carried out on ulcerative skin lesions. The avidin-biotin-peroxidase complex (ABC) technique was used for the immunohistochemical studies performed on paraffin sections. The panel of antibodies used in this study included AE-1 and Cam 5.2 (anti-low molecular weight cytokeratins; Dako, Glostrup, Denmark), S-100 (Dako), anti-α-actin (Dako), HHF 35 (anti-actins), anti-desmin (Dako), anti-vimentin (Dako), anti-light and -heavy immunoglobulin chains (Dako), and anti-CD19, -CD20, -CD21, -CD45R, and -CD45RO (Dako). Briefly, after removal of paraffin and rehydration, endogenous peroxidases were blocked with 0.3% H_2O_2 in methanol. Then the samples were incubated with mouse or rabbit primary antibodies for 10 to 12 hours at 4°C. Biotinylated anti-mouse and anti-rabbit immunoglobulins (Dako) were used as secondary antibodies followed by incubation with avidin-biotin-peroxidase conjugates and development in diaminobenzidine (Sigma Chemical Co., St. Louis, MO). Morphological characterization of lymphomas was carried out according to the Standard Murine Lymphoma Classification.[38] BKV TAg was detected on sections of frozen tissues by indirect immunofluorescence using a first serum to TAg derived from hamsters bearing tumors induced by BKV-transformed cells and a second rabbit serum to hamster IgG conjugated with fluorescein isothiocyanate.

Electron Microscopy

For ultrastructural investigations, tumors were fixed with glutaraldehyde in PBS (0.2 mol/L, pH 7.2) for 8 hours, post-fixed in 1% OsO_4 in PBS for 4 hours, dehydrated, and embedded in Araldite. Ultrathin sections were stained with uranyl acetate and lead citrate and then examined in a Hitachi H-7000 electron microscope.

Southern Blot Hybridization and Reverse Transcriptase-Polymerase Chain Reaction (RT-PCR)

Southern blot hybridization was carried out according to standard techniques,[39] using BKV/*tat* (pRPU3Rtat) recombinant DNA as a probe labeled with ^{32}P by nick translation to a specific activity of 1×10^9 to 6×10^9 cpm/μg, as previously reported.[36]

RT-PCR was used for amplification of BKV early region and *tat*, as previously described.[36] Reverse transcription

of total cytoplasmic RNA was carried out with the commercial kit provided by Invitrogen (San Diego, CA), according to the manufacturer's instructions. Two 23-mer oligonucleotides (5′-TAGGTGCCAACCTATGGAACAGA-3′ and 5′-GAAAGTCTTTAGGGTCTTCTACC-3′) were used to amplify a 180-bp sequence of BKV early region, whereas a 21-mer oligonucleotide (5′-GAAGCATCCAGGAAGTCAGCC-3′) and a 24-mer oligonucleotide (5′-ACCTTCTTCTTCTATTC-CTTCGGG-3′) were used to amplify a 239-bp sequence of *tat* cDNA. The amplified products were hybridized with an internal BKV DNA oligonucleotide probe (5′-AATCT-TCATCCCATTTTTCA-3′) or the complete *tat* cDNA labeled with ^{32}P by polynucleotide kinase.[36]

Results

Presence and State of the Transgene DNA and Expression of tat and BKV Early Region in Tissues of Transgenic Mice

To detect the transgene, DNA extracted from tails of the seven founder mice was doubly digested with *Bam*HI and *Eco*RI, which produce four fragments on pRPU3R*tat*, the transgenic plasmid containing BKV early region and *tat* DNA.[36] The restricted DNAs were then subjected to Southern blot hybridization. All founder mice showed the presence of the four *Bam*HI/*Eco*RI fragments and of additional hybridization bands related to integration of pRPU3R*tat* into flanking host DNA sequences (data not shown). The molar ratio of the four restriction fragments, measured by densitometric analysis, indicated a number of pRPU3R*tat* molecules ranging from 10 to 50 copies/cell. Moreover, the results were suggestive of a single integration even of multiple copies of pRPU3R*tat* arranged in a tandem array. All generations of transgenic mice obtained by mating animals belonging to the same transgenic line stably maintained this hybridization pattern. All tissues and organs in each transgenic line showed the presence of the pRPU3R*tat* DNA as tandem insertions in a variable number of copies (5 to 20) per cell (Figure 1). *tat* and BKV RNA were detected in all tissues and in primary tumors of the transgenic mice by RT-PCR (Figure 2, A and B) with the exception of lung, which was negative for *tat* RNA. *tat* and BKV DNA and RNA were never detected in normal control mice, as expected, because mice, contrary to humans, do not bear a BKV latent infection. In addition, polyoma virus, which produces a latent infection in mice, is not homologous to BKV sequences. As previously reported,[36] BKV TAg was constantly detected by immunofluorescence as a nuclear granular staining in tumors and organs (liver, lung, kidney, brain, and skin) of transgenic mice (data not shown).

Phenotypes Manifested in BKV/tat Transgenic Mice: Pathological Findings

A number of phenotypes were observed in homozygous and heterozygous transgenic animals with no differences between the two groups. A total of 171 transgenic mice

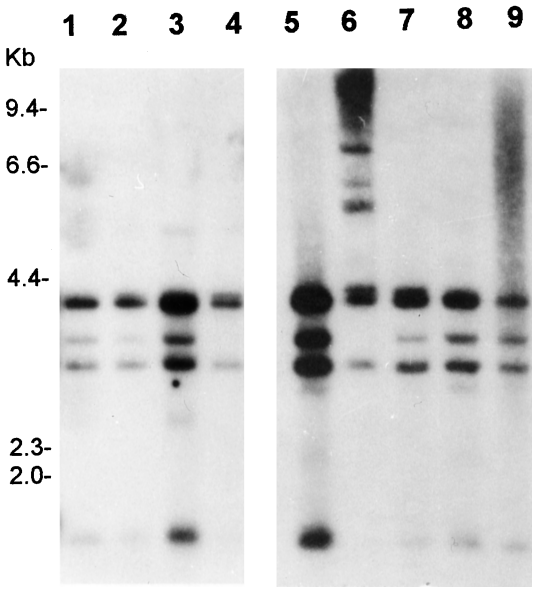

Figure 1. Analysis of the presence of the pRPU3Rtat transgene DNA in tissues of transgenic mice. Total cellular DNA (10 μg) was digested with *Bam*HI and *Eco*RI and analyzed by Southern blot hybridization. The double digestion generates four fragments on pRPU3Rtat. Lane 1, control plasmid pRPU3Rtat (10 genome equivalents per cell); lanes 2 to 9, DNAs from intestine, skin, liver, lung, brain, kidney, stomach, and spleen, respectively. The position of molecular weight fragments, derived by digestion of λ-phage DNA with *Hin*dIII, is indicated on the left.

(135 BDF homozygotes and 36 BDF × CD1 hybrids) and 400 control animals were subjected to autopsy and histological examination of all organs. All transgenic animals were affected by lesions, whereas in BDF and BDF × CD1 control mice, only 44 of 400 animals (11%) devel-

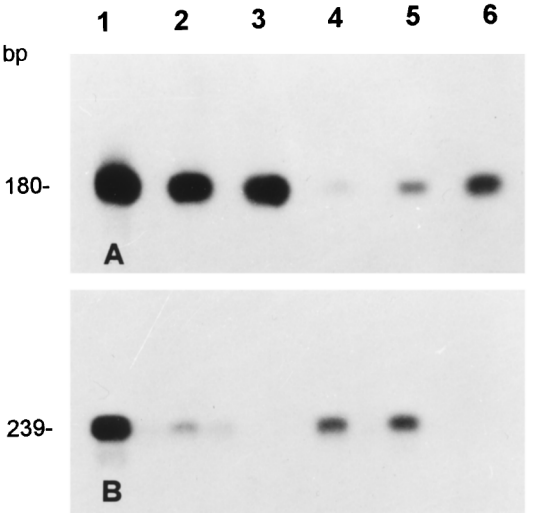

Figure 2. Analysis of the expression of BKV early region and *tat* by RT-PCR. RNAs were extracted from tissues and transcribed into cDNA by reverse transcription. The cDNAs were amplified by PCR, migrated on 2% agarose gel, and hybridized to a ^{32}P-labeled oligonucleotide probe internal to BKV early region (A) or to a complete ^{32}P-labeled *tat* cDNA (B). A: Lane l, BKV early region amplified as a control by RT-PCR from the T53 cell line, constitutively expressing BKV TAg and *tat*[36]; lane 2, kidney; lane 3, skin; lane 4, lung; lane 5, brain; lane 6, liver. B: lane 1, *tat* amplified as a control by RT-PCR from the T53 cell line; lane 2, kidney; lane 3, lung; lane 4, liver; lane 5, skin; lane 6, RT-PCR solution without RNA.

Table 1. All Types of Lesions Observed in BKV/*tat* Transgenic and Control Mice

Animals	Transgenic mice with lesions	Control mice with lesions
BDF	135/135 (100%)	38/316 (12.0%) $P < 10^{-38}$
BDF × CD1	36/36 (100%)	6/84 (7.1%) $P = 10^{-25}$
Total	171/171 (100%)	44/400 (11.0%) $P < 10^{-38}$

P = probability by Fisher's exact test.

oped lesions. A total of 282 and 68 lesions arose in transgenic and control animals, respectively (Table 1).

Types of Lesions

The lesions observed in transgenic and in control mice were grouped in three morphological categories: 1) tumors, 2) hyperplastic and dysplastic lesions, and 3) non-neoplastic lesions. This last group included two subtypes: 1) specific lesions and 2) secondary lesions. Specific lesions were observed almost exclusively in transgenic animals, whereas secondary lesions were caused by other illnesses such as chronic infections and tumors or were unrelated to the experimental conditions (spontaneous lesions).

Tumors

Fifty tumors (29.2%) were observed in transgenic mice (Table 2), and more than one type of tumor was frequently present in the same animal. The majority of the neoplasms were malignant, invasive, and producing metastases, except for benign hemangiomas of the liver. In control animals, 15 tumors (3.7%) of only two histotypes were found: adenocarcinomas of the skin glands and lymphomas (Table 2). In control mice, lymphomas were invariably detected in the oldest animals. In transgenic and control animals, tumors appeared both in males and females.

In transgenic mice, the skin with the adnexes, the eyes, the liver, the rectum, and the lymphoid system were the most frequently involved organs. These tissues also showed hyperplastic and dysplastic alterations associated with tumors, and tumors manifested an early onset in younger animals compared with control mice. These results are consistent with a greater frequency and a wider range of phenotypic alterations in transgenic mice than in control mice.

Skin Adenocarcinomas

These tumors showed a nodular growth pattern with great invasiveness in the adjacent tissues. The tumor cells appeared undifferentiated with scarce basophilic cytoplasm and enlarged hyperchromic nucleus (basaloid cells, Figure 3A). Chromatin granules were adherent to the nuclear membrane, and nucleoli were often evident. PAS reaction for cytoplasmic mucins was constantly negative. More differentiated zones consisted of 1) tubular or glandular structures lined by epithelial cells with apocrine secretion features (cytoplasmic blebs of secretion) and differentiation and 2) large cystic spaces resulting from the confluence of glandular structures and sometimes containing prominent papillae lined by epithelial apocrine cells. The ratio between differentiated and undifferentiated zones was variable with slight prevalence of the undifferentiated ones. Immunohistochemical reactions confirmed the histological diagnosis showing strong reactivity to CAM 5.2, AE-1, and S-100 antibodies in the cytoplasm of the neoplastic cells. Ultrastructural observations demonstrated numerous lumens lined by microvilli. The neoplastic cells showed blebbing apical cytoplasm and tight junctions of the membrane and contained rough endoplasmic reticulum, mitochondria, and large electron-dense secretory granules, 300 to 800 nm in size, that resembled lysosomes (Figure 3B). Skin adenocarcinomas in control mice were very similar to those observed in transgenic mice, except that they appeared in a significantly lower proportion of animals (Table 2).

Table 2. Tumors Observed in BKV/*tat* Transgenic and Control Mice

Tumor histotype	Transgenic mice		Control mice	
	Number	Percentage*	Number	Percentage*
Skin adenocarcinoma	13	7.6	6	1.5 $P = 10^{-4}$
Skin squamous cell carcinoma	3	1.7		
Leiomyosarcoma	10	5.8		
Hepatoma/hepatocarcinoma	5	2.9		
Liver hemangioma	4	2.3		
Lymphoma	13	7.6	9	2.2 $P = 10^{-3}$
Lung carcinoma	1	0.6		
Lipoma	1	0.6		
Total	50	29.2	15	3.7 $P = 10^{-17}$

*The percentage is related to the total of transgenic mice (171) and control mice (400), respectively. P, probability by Fisher's exact test.

Skin Squamous Cell Carcinomas

Three tumors of the skin observed in transgenic mice belonged to this group; two were deeply located nodular tumors, and one had a verrucous esophitic appearance. Neoplastic cells situated in the periphery had scarce basophilic cytoplasm and large hyperchromatic nuclei like basal-type epidermal cells, tending to a progressive maturation toward the center of the tumor nodule (Figure 3C). In the center of the tumor, where the differentiation was completed, squamous cells, horny cysts, and keratin scales were observed. One of the tumors presented abrupt squamous maturation of the basal-like cells with a large amount of keratinized necrotic cells and numerous shadow cells often associated with an inflammatory reaction with multinucleated reactive giant cells in the stroma. Infundibular keratin cysts were associated with this morphological pattern.

Leiomyosarcomas of the Skin

These tumors were found only in transgenic mice and showed monotonous features and localization in the deep dermis or hypodermis. Histologically, the tumors were formed by spindle cell bundles irregularly oriented and often interlaced with whirling features around the vessels. The tumor cells showed spindle nuclei with smooth borders (Figure 3F); their cytoplasm was large with fibrillar eosinophilic structures and externally outlined by a thin PAS-positive basal lamina. Variations of cell size and grading of differentiation were evident and related to the mitotic activity that was very intense in the zones where cytological atypias and bizarre plurinucleated cells were more frequent. Infiltrative growth pattern and invasion of the adjacent muscular and bone tissue were independent from the differentiation. The tumor cell immunophenotype showed reaction with the antibody HHF-35 and with antibodies to actin, desmin, and vimentin, according to the leiomuscular nature of these neoplasms. Electron microscopic examination showed an undifferentiated pattern of tumor cells and constantly the external basal lamina. Small and irregular bundles of actin filaments sometimes running parallel to the long axis of the cell were seen in the cytoplasm, with rare dense bodies beneath the cytoplasmic membrane, typical of this type of tumor.

Hepatomas/Hepatocarcinomas

All five liver cell neoplasms observed had a nodular architecture with a variable degree of differentiation from the most differentiated adenoma-like to the most aggressive tumors. No fibrous septa divided the neoplastic nodules from the adjacent normal liver tissue (Figure 3D). The most differentiated tumors were formed by epithelial plates irregularly oriented and anastomosized, separated by sinusoids and containing two or more hepatocyte-like cells, simulating normal liver architecture (Figure 3E). In the most undifferentiated zones, the cells showed marked atypia (large amphophilic cytoplasm, vesicular nuclei and nucleoli), irregular vascularization with thrombosis, and frequent necrosis. Eosinophilic bodies were frequently evident in the cytoplasm of the hepatocyte-like tumor cells.

Cavernous Hemangiomas

This was the only benign tumor of the liver consisting of irregular vascular lacunae, separated by hepatocyte plates or by fibrous-myxoid septa lined by flat endothelial cells, with luminal or mural thrombosis.

Lymphomas

The majority of these tumors involved abdominal lymph nodes, spleen, sometimes liver, kidneys, lungs, and bone marrow. Lymph nodes were enlarged and packed by pericapsular extension of tumor proliferation. The spleen showed doubled volume and on the cut surface numerous white lymphoid nodules often fused together. White neoplastic nodules were also found in the liver, kidneys, and lungs. Histologically, lymphomas showed a diffuse growth pattern with residual nodular features and consisted of a mixture of follicular center cell types (Figure 3G). The neoplastic cells expressed CD19, CD20, CD21, and CD45R (4KB5) B-cell-specific markers, confirming that these tumors are B-cell follicular center lymphomas. No differences were observed in cytological composition, organ involvement, and diffusion between lymphomas of transgenic mice and those of controls, except that lymphomas in control mice involved a significantly lower percentage of animals (Table 2) and always appeared later, in the oldest animals, as compared with transgenic mice. These tumors in both groups of animals were frequently associated with amyloid deposits in the spleen, liver, and kidneys.

Hyperplastic and Dysplastic Lesions

A number of hyperplastic and dysplastic phenotypes were histologically observed significantly more frequently in transgenic animals than in controls (Table 3). Most of these alterations involved the skin or its adnexes and were obvious at birth or appeared later in life. Liver and rectum were the other organs frequently involved. Except for skin lesions, which were observed only in males, all of the other alterations affected indifferently males and females.

Skin Lesions in Transgenic Mice

A great number of transgenic animals were hairless at birth and remained with scarce fur until 2 months of age. Over denuded areas of the skin some of them developed squamous cell hyperplasia and hyperkeratosis. Several animals remained of small size and underdeveloped up to 2 months of age. Other animals developed areas of alopecia in specific sites, that is, on the back, nose, and circularly around eyes in a spectacle-like fashion. Most

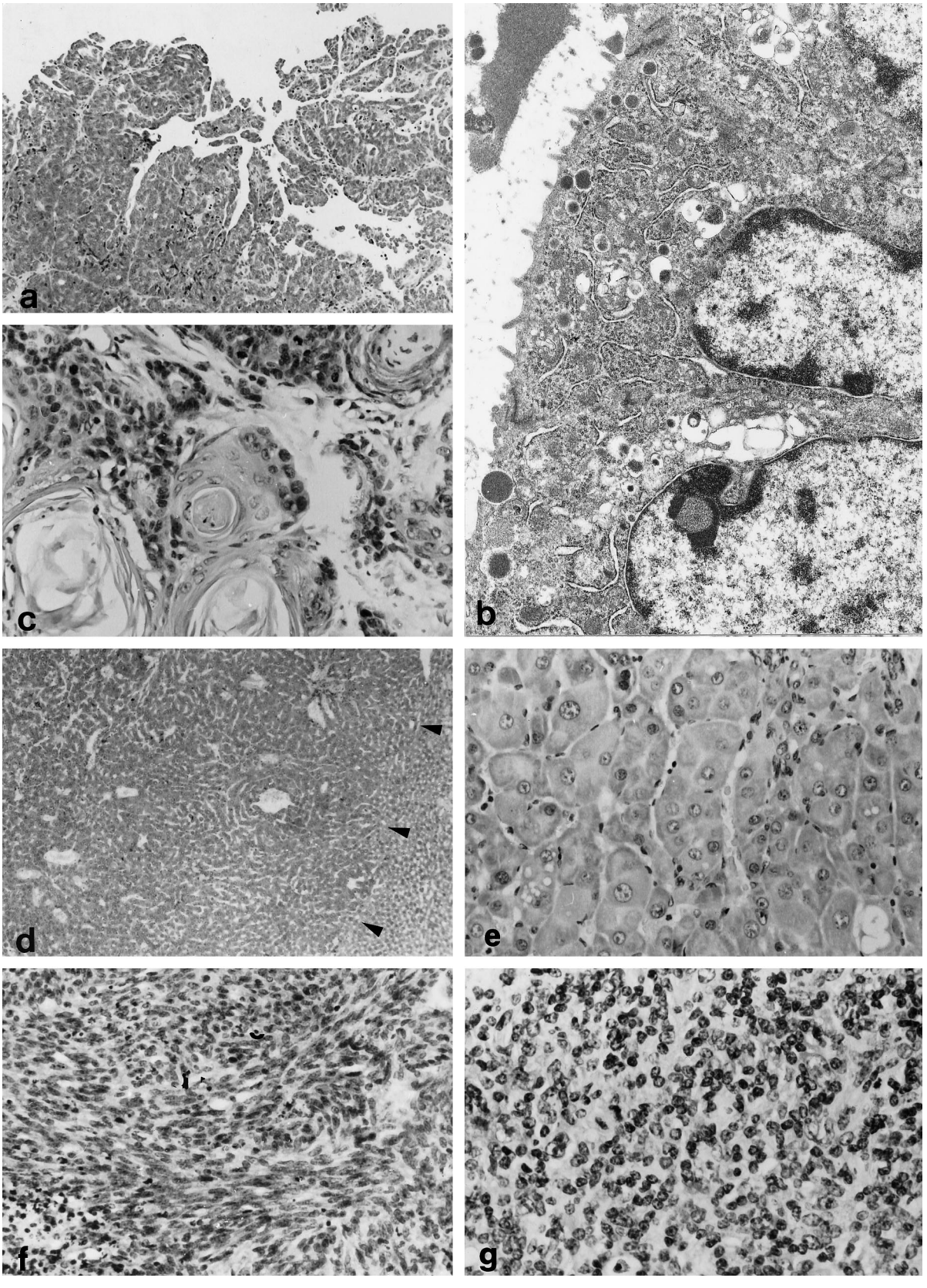
a
b
c
d
e
f
g

Table 3. Hyperplastic/Dysplastic and Non-Neoplastic Lesions Observed in BKV/*tat* Transgenic and Control Mice

Hyperplastic/dysplastic lesions	Transgenic mice		Control mice	
	Number	Percentage*	Number	Percentage*
Skin hyperplasia and neoangiogenesis	41	24.0	7	1.7 $P = 10^{-17}$
Skin, liver, and kidney cysts	20	11.6	1	0.2 $P = 10^{-10}$
Liver hyperplasia and dysplasia	29	17.0	4	1.0 $P = 10^{-12}$
Rectum polyps and prolapse	16	9.3		
Eye lesions	18	10.5	1	0.2 $P = 10^{-9}$
Non-neoplastic lesions				
Amyloidosis	51	29.8	26	6.5 $P = 10^{-12}$
Hydronephrosis and pyelonephritis	32	18.7	13	3.2 $P = 10^{-9}$
Myocardium infarct	16	9.3		
Liver inflammation	13	7.6	1	0.2 $P = 10^{-6}$

*The percentage is related to the total of transgenic mice (171) and control mice (400), respectively. *P*, probability by Fisher's exact test.

prominent was a thickening of the skin followed by ulcerations, often associated with hemorrhages (Figure 4, A and B). These lesions were more frequent and appeared much earlier in cross-bred BDF × CD1 mice than in mice of the BDF strain. Skin thickening and ulceration were localized in the back of the animals and appeared exclusively in males, both in BDF and BDF × CD1 cross-bred mice, whereas all the other lesions affected indifferently males and females. Trauma from fighting was excluded as a cause of skin lesions because isolated animals also had identical skin changes. All lesions described above were reversible. The lesions lasted generally 1 to 2 months and then healed, and animals returned to normality. Even the most dramatic ulcerative lesions were completely cured. Histologically, we identified three evolving steps, a short opening lesion, the ulcer, and a reparative healing phase.

Opening Phase Lesions

The lesions preceding the skin ulcers appeared as focal overgrowth of the epidermis with hyperkeratosis and acanthosis and were constantly associated with interstitial edema and myxoid change of the ground substance of perivascular and periadnexial spaces, causing the detachment of the dermal/epidermal junction. A subepidermal bulla was evident in the largest lesions. The last phase consisted of detachment of skin strips (1 or 2 cm long) denuding the underlying dermis. The adjacent capillaries were ectasic and the derma was edematous without increase of inflammatory cells or fibroblasts.

Ulcerative Lesions

Overt skin ulcers presented with variable size and extension into the dermis and sometimes into the hypodermis. They were often covered by a thick crust or by a necrotic exudate consisting of neutrophil leukocytes and nuclear and keratin debris. The bed of the ulcers was formed by granulation tissue with abundant capillaries in a fibromyxoid background infiltrated by inflammatory cells (macrophages, lymphocytes, and leukocytes) and activated fibroblasts. Neoangiogenesis was very intense during the first reparative phase simulating a neoplastic Kaposi's sarcoma-like proliferation (Figure 4, C–E). The lesions were characterized by dermal hypercellularity consisting of a proliferation of spindle-shaped cells and endothelial cells. The endothelial cells showed cytoplasmic vacuoles prone to fuse and to form a small lumen. Slit-like spaces and round capillaries lined by a single or two flat endothelial cells gradually appeared at the periphery of the lesions. In the more advanced ulcerative lesions, inflammation was more evident and the reparative granulation tissue, consisting of a neoformed capillary network, was more prominent. The numerous fibroblasts interposed among the capillaries did not show nuclear atypias or mitosis. The ratio and the distribution of capillaries and fibroblasts showed a linear relationship with the evolution of the lesions with a progressive increase of the fibroblast bundles in the latest phases. The regression phase was represented by a progressive decrease of blood capillaries and inflammation with increase of collagen fibers.

Reparative Phase Lesions

Skin ulcers underwent complete reconstruction of the epithelium, and this phase appeared as a flat or depressed sub-atrophic lesion lined by hyperkeratotic epidermis (Figure 4F). The underlying dermis developed a reparative tissue consisting of fibroblast bundles with irregular orientation and scarce capillaries, containing residual inflammatory cells, such as macrophages, sometimes melanophages, lymphocytes, and plasma

Figure 3. Tumors in transgenic mice: **A**: Poorly differentiated skin adenocarcinoma consisting of solid pseudo-papillary fronds. H&E; magnification, ×63. **B**: Ultrastructurally, the neoplastic cells show apocrine-type markers such as apical membrane bleb-like protrusions and secretory electron-dense granules. Pb&Ur; magnification, ×12,000. **C**: Skin squamous cell carcinoma characterized by cords and nests of basaloid cells with abrupt squamous differentiation. H&E; magnification, ×100. **D**: Hepatoma. No fibrous capsule separates hepatoma from normal liver parenchyma. Lobular architecture is lost, although hepatoma cells are still arranged in plates surrounded by fibrous tissue containing capillaries but no sinusoids. **E**: Hepatocarcinoma cells are larger with atypical nuclei forming glandular-like structures. H&E; magnification, ×25 **D** and ×160 (**E**). **F**: Skin leiomyosarcoma diffusely infiltrating dermis and hypodermis is formed by fascicles of spindle cells with characteristic blunt nuclei. H&E; magnification, ×100. **G**: Follicular center lymphoma of mixed cell type, consisting of a heterogeneous lymphoid cell population and rich in mitoses. H&E; magnification, ×250.

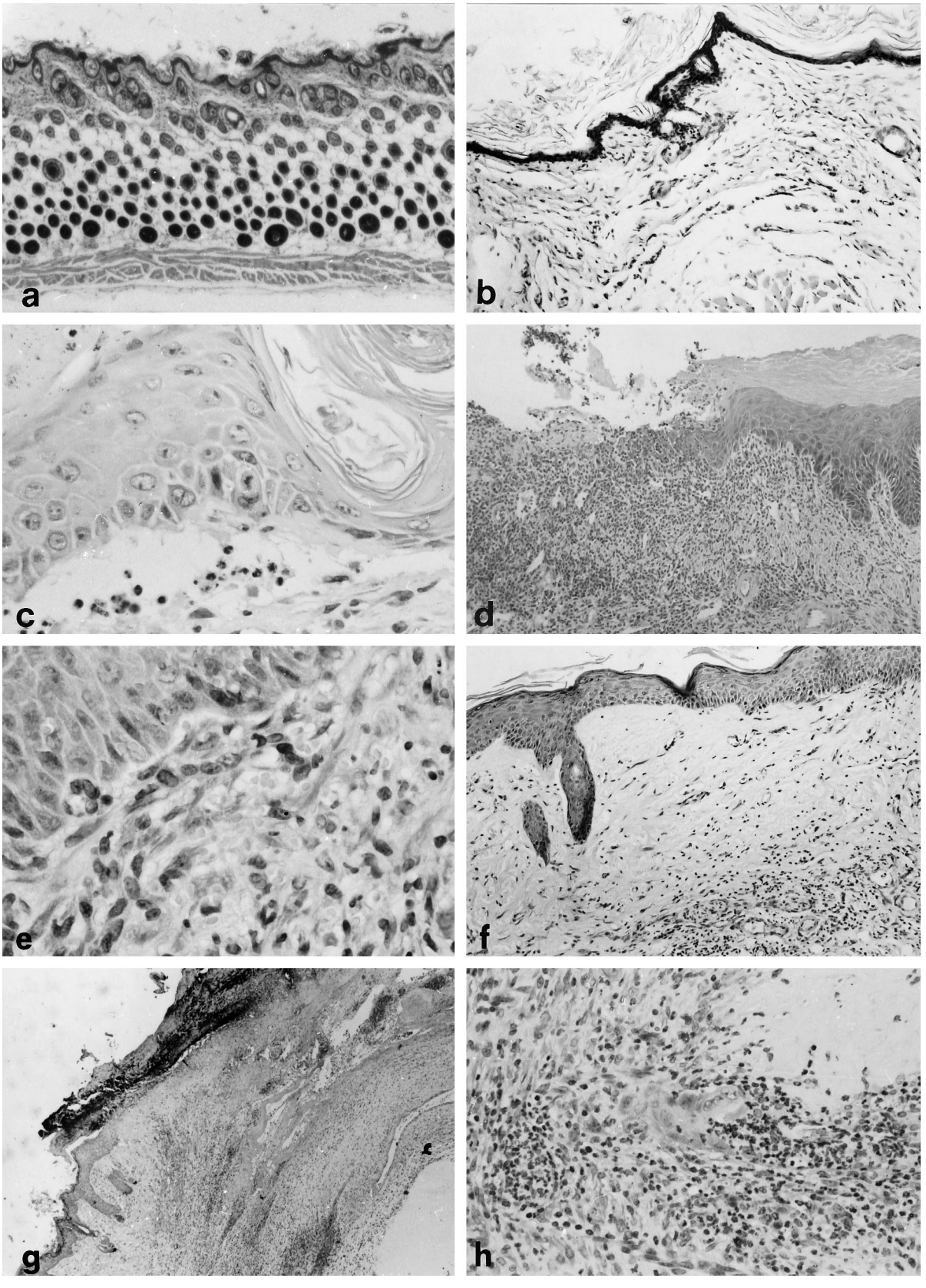
a
b
c
d
e
f
g
h

cells, located in perivascular spaces. In numerous animals, persistent foci of inflammatory reaction were associated with hair debris in the dermis. In the deep subcutaneous tissue, chronic suppurative inflammatory foci with hair debris or with dilated hair infundibula were sometimes found. These inflammatory lesions underwent progressive substitution with reparative granulation tissue and fibroblastic bundles with fibrous collagen tissue, similarly to late cicatrization processes. Skin lesions, independently from the evolution, were frequently associated with hyperplastic and regenerative modifications of the liver.

Skin Lesions in Control Mice

Only 7 (1.75%) control animals of the BDF strain showed this type of lesion. The ulcers differed from the lesions of transgenic mice for these characteristics: 1) they never appeared at birth and always developed in adult mice, both males and females; 2) the ulcers showed abrupt onset with detachment and formation of skin flaps; they progressively enlarged and were covered with necrotic exudate; 3) the inflammations, likely due to bacterial infections, were purulent in nature and seemed to arise from the hair follicles with secondary confluence and constant extension to the subcutis; and 4) reparative granulation tissue appeared late, and all the reparative phases had slow progression and long duration (Figure 4, G and H). During this phase, proliferation of fibroblasts and myofibroblasts was not as intense as observed in transgenic mice.

Cystic Lesions

Cysts of the skin, liver, and kidneys were observed rather frequently (11.6%) in transgenic mice, whereas they were uncommon (0.2%) in control animals (Table 3). Cyst development may be related to a dissociation of cell growth and differentiation, due to a delay in cell loss. In the skin, the abnormal persistence of differentiated elements and the increased number of cells cause a progressive enlargement of the hair or gland infundibulum up to the cyst development.

Liver Lesions in Transgenic Mice: Hyperplastic/Dysplastic (H/D) Lesions of Hepatocytes

The overall normal liver architecture was not altered. The H/D lesions were cytological alterations of hepatocytes evenly distributed and detectable only by microscopic observation. No fibrous or wall delimitations could be found, and the ratio between normal and H/D liver cells was variable in the animals examined. The nuclear modifications found in mice with other pathological conditions (hepatitis or amyloidosis) were not considered as dysplastic and therefore are not evaluated in this section. The H/D cells showed great polymorphism with intense basophilic and larger cytoplasm (twice than normal), central nuclei with prominent nucleoli, and chromatin clumps with great variability in size (Figure 5, A and B). These modifications were graded as follows: 1) low-grade H/D lesions with slight increase in nuclear size up to twice normal, scarce evidence of nucleoli, N/C ratio lower than 1, and involvement of less than 50% of the cells; 2) moderate-grade H/D lesions with increased nuclear size twice or more than twice normal, clear evidence of nucleoli, and binucleation in more than 50% of the cells; 3) severe-grade H/D lesions with prominent variability of nuclear size and presence of bizarre and giant nuclei in a background of cytological modifications and N/C ratio greater than 1. Only the moderate and severe grades of H/D alterations were considered to be related to the transgenic phenotype, whereas the low-grade H/D modifications were regarded as reactive conditions. Additional findings were Küpffer cell hyperplasia and occasional lymphocyte infiltrates in the portal space. In the liver with hepatic tumors other than hemangiomas the adjacent liver cells showed a variable grade of H/D lesions from moderate to severe, suggesting that these lesions may represent preneoplastic areas of the liver where hepatomas and hepatocarcinomas started their growth.

Liver Hyperplasia in Control Mice

Morphological alterations of hepatocytes similar to the moderate-grade H/D lesions observed in transgenic animals was found in four control mice (1%). More severe alterations were never detected. Regenerative hyperplasia with variable size of hepatocyte nuclei was regularly associated with liver amyloidosis and phlogosis.

Rectum Lesions: Mucosal Polyps and Prolapse

Prolapses of the rectal mucosa caused pedunculated polyps of 0.7 to 2.5 cm in length (peduncle of 0.3 to 0.5 cm) consisting of histologically exaggerated mucosal outfolding with extrusion of muscularis mucosa and submucosa (Figure 5, C and D). The mucosa formed the polyp head and the muscularis mucosa the peduncle. Small superficial ulcerations were constantly found covered by necrotic exudate; the glands were elongated, tortuously branched, and lined by eosinophilic and clear mucinous cells. The basal regenerative part of the crypts

Figure 4. Hyperplastic and dysplastic skin lesions: A: Normal-haired skin of a control animal with numerous hair follicles in the dermis. H&E; magnification, ×25. B: Zone of alopecia in the skin of a transgenic mouse with complete absence of hair and with increased fibrous tissue in the dermis. H&E; magnification, ×63. C to F: Ulcerative lesions of the skin in transgenic mice. C: Opening phase with squamous cell hyperplasia of the epidermis and detachment of dermal/epidermal junction. H&E; magnification, ×250. D: Ulcerative phase with inflammatory infiltrate. H&E; magnification, ×63. E: Proliferation of fibroblastic-like cells and Kaposi-like neo-angiogenesis in the derma. H&E; magnification, ×250. F: Reparative phase with complete re-epithelialization of the ulcer, disappearance of inflammatory infiltrate and newly-formed capillaries by fibrous tissue. H&E; magnification, ×63. G and H: Ulcerative skin lesions in control animals; ulcer of the epidermis is covered by necrotic exudate and inflammatory suppurative infiltrate diffusely in the dermis and the hypodermis. H&E; magnification, ×25. H: Residual of hair follicle with features of suppurative folliculitis. H&E; magnification, ×160.

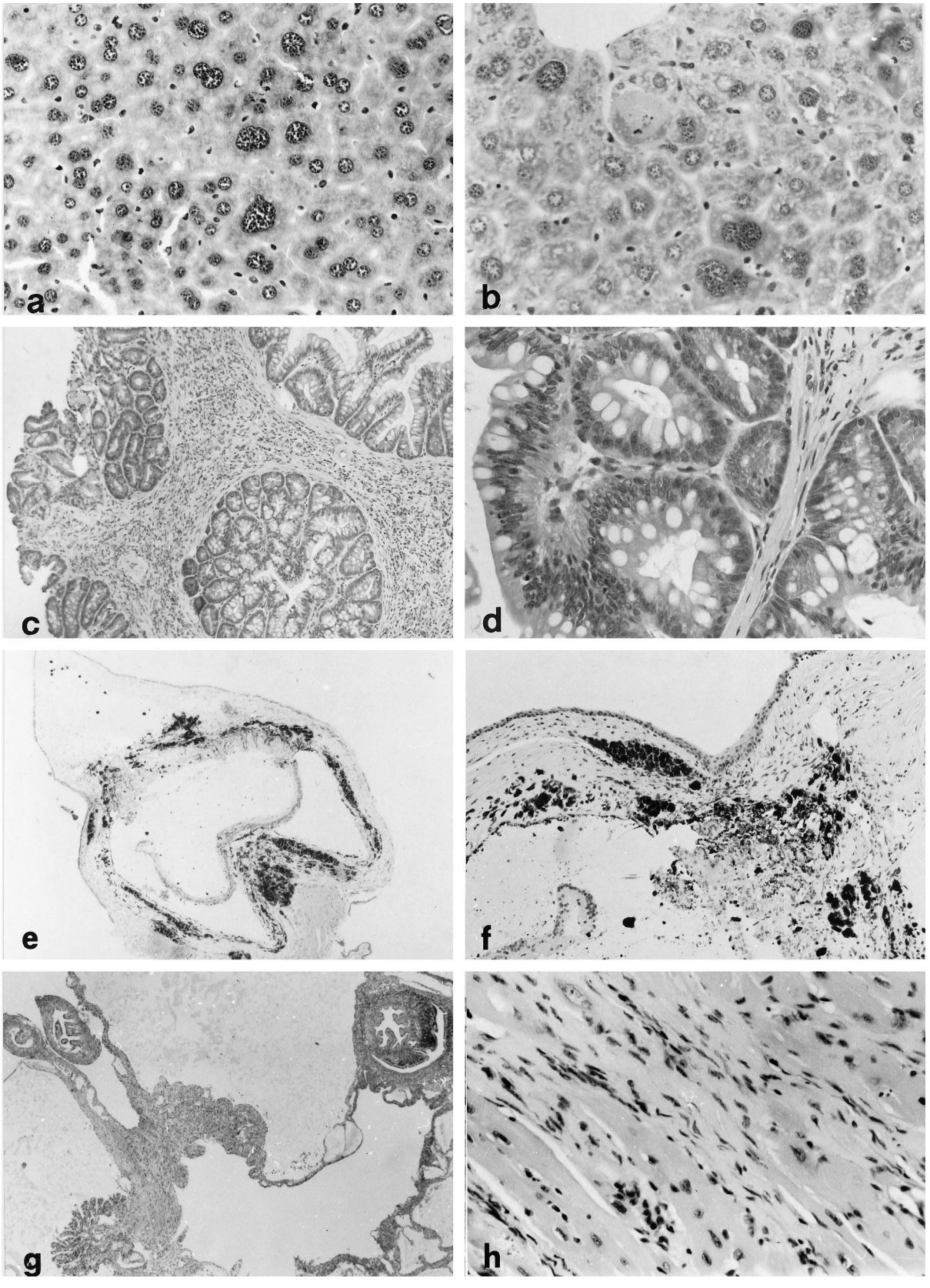
a
b
c
d
e
f
g
h

was not amplified, and the count of mitoses was normal. Mucinous cells were more numerous in the superficial zones of the hyperplastic crypts. Distribution of the hyperplastic glands was heterogeneous and always related to the reparative and regenerative processes, secondary to the mucosal ulcerations and probably triggered by the intense lymphocyte and monocyte infiltrates. Bundles of muscularis mucosa fibers and ectasic vessels were constantly present in the stroma. These alterations were observed only in transgenic animals (Table 3).

Adjacent Anal Skin

The anal orifice and the adjacent skin were lined by hyperplastic squamous cell epithelium with acanthosis and elongated, deep rete ridges; the dermis was edematous and contained an increased amount of fibroblasts and perivascular lymphocyte/monocyte cuffings (Figure 5G). Infundibular and pilo-sebaceous cysts were frequently associated with rectal prolapses, often progressing to suppurative abscesses. The cut surface appearance of these lesions was very similar to infiltrative neoplasia.

Eye Lesions

A substantial proportion of transgenic animals developed eye lesions that affected the lens, cornea, posterior chamber, and retina with a degenerative process associated with inflammation (Figure 5, E and F). The eye disease became progressively more severe and most often ended in blindness. The lens showed cataract formation, and this alteration was often associated with corneal ulcerations that were complicated by inflammation of the iris and ciliary body. This last condition induced retrocorneal fibrosis, lens dislocation, degeneration, and disruption of iris tissue by infiltration of inflammatory cells. The lesions of deep eye tissues involved detachment of the retina, choroid hemorrhages, and inflammatory infiltration, with the features of an endo-ophthalmitis. Reparative fibrosis followed as an end step with accumulation of macrophages, melanophages, and hemosiderin granules and entrapment of retinal membrane fragments and iris residuals.

Non-Neoplastic Lesions

Amyloidosis

Systemic amyloidosis represented the most frequent non-neoplastic and nonspecific alteration observed in transgenic as well as in control animals (Table 3). It was always associated with chronic inflammation of the skin, kidneys, liver, or the pelvic organs in females. Amyloid substance depositions were commonly found in the liver, kidneys, and spleen and less frequently in the small intestine wall and in lymph nodes. The most common macroscopic aspect was organomegaly. In the liver, amyloid accumulated in the Disse's spaces causing compression and atrophy of the liver cells. In kidneys, amyloid deposition was observed in glomeruli and in the wall of arterioles; in spleen, the amyloid appeared as an interstitial accumulation of a hyaline substance around the arterioles with complete distortion of the normal architecture.

Chronic Inflammatory Lesions and Abscesses

Chronic suppurative inflammations were more frequent in transgenic mice (up to 30%) than in control animals (3.5%) and were more commonly localized in subcutis and in the kidneys than in other sites (as the rare suppurative salpingitis-oophoritis). Reactive systemic amyloidosis generally accompanied these suppurative lesions. Subcutaneous abscesses were related to the secondary inflammation of the infundibulum-sebaceous cysts and were often localized in the posterior leg or in the perianal region. Hydronephrosis was consistently associated with inflammation and interstitial fibrosis of the kidneys; the grade of parenchymal atrophy was variable, but sometimes severe (Figure 5G). Liver involvement in inflammatory processes was generally observed as an infiltration of portal spaces.

Heart Lesions

Symmetric left ventricular hypertrophy was more common in transgenic mice than in control animals; this condition was generally associated with small fibrous scars of the myocardium especially in animals older than 1 year. Large myocardial scars, a probable outcome of myocardial infarction, with irregular shape, consisting of fibrous tissue and residual perivascular inflammatory infiltration, were found only in transgenic mice (Figure 5H; Table 3).

Discussion

The introduction of the pRPU3R*tat* plasmid, containing BKV early region and HIV-1 *tat* gene, into the mouse germ line led to the development of seven lines of transgenic mice. Different phenotypes appeared in mice bearing the BKV/*tat* transgene independently from homozygosis (BDF1) or heterozygosis (BDF1 × CD1) of the transgenic strains. These phenotypes included tumors as

Figure 5. Hyperplastic/dysplastic and non-neoplastic lesions in transgenic mice. **A** and **B**: Hyperplastic/dysplastic modifications of hepatocytes consisting in atypical nuclei of increased size, prominent nucleoli, and mitoses. **A**: Cell dysplasia of moderate grade. H&E; magnification, ×160. **B**: Cell dysplasia of severe grade. H&E; magnification, ×160. **C** and **D**: Rectal polyps consisting of mucosal prolapse with hyperplasia of the glands showing irregular branching and lined by hypersecretive mucinous cells. Epithelial cells show crowding and vertically oriented nuclei without atypical figures. H&E; magnification, ×63 (**C**) and ×160 (**D**). **E** and **F**: Eye lesions: panophthalmitis with reduction of the eye volume, disappearance of ciliary body, detachment and dislocation of the retina, and diffuse infiltration by pigmented cells. H&E; magnification, ×25 (**E**) and ×63 (**F**). **G**: Hydronephrosis with cyst-like spaces delimited by thin fibrous walls containing residual glomeruli. H&E; magnification, ×25. **H**: Myocardial scar consisting of fibrous tissue separating and replacing muscle cells. H&E; magnification, ×160.

well as hyperplastic/dysplastic lesions and non-neoplastic alterations, with involvement of many organs. Only a small proportion (11%) of control animals showed a total of 68 lesions, whereas all of the transgenic mice were affected, with a total of 282 lesions. In this transgenic mouse model, we observed dermal lesions, similar to the early phases of Kaposi's sarcoma, skin tumors (adenocarcinomas, leiomyosarcomas, and squamous cell carcinomas), lymphomas, hepatomas, hepatocarcinomas, hyperplastic/dysplastic lesions, and polyps of the rectal mucosa. Such results indicate multiple targets of the transgene activity.

The incidence of tumors was not very high in BKV/*tat* transgenic mice (29.2%), but statistically significant as compared with the tumor frequency in controls (3.7%; $P = 10^{-17}$). The low incidence of tumors suggests that the transgene is not sufficient to induce a full oncogenic process and that other cooperative events are necessary for the development and/or progression of the tumor phenotype. In addition, the presence of more than one type of tumor in the same animal, although other animals were tumor-free, suggests individual variations in the expression of the transgene. This may be due to position effects, dependent on the integration of the transgene in different sites of the genome in different animals, thus receiving a variable influence on expression by the endogenous transcriptional enhancers or silencers of the host.

As in *tat* transgenic mice,[35] skin tumors are predominant in BKV/*tat* transgenic mice, except that they showed different histotypes. In *tat* transgenic mice, only fibrosarcomas were observed. They arose over the skin lesions, apparently as a progressive process of dermal alteration initiated by spindle cell proliferation.[35] In BKV/*tat* transgenic mice leiomyosarcomas, squamous cell carcinomas and adenocarcinomas were observed. Only adenocarcinomas developed in controls, but with very low incidence. These tumors did not arise over the skin lesions and were not related to them. Thus, BKV/*tat* and *tat* transgenic mice have the skin as a common target organ. However, in BKV/*tat* transgenic mice the oncogenic process involves more than one cell type, with a consequent appearance of a variety of tumor histotypes.[36]

In *tat* transgenic mice, 42.2% of male animals showed proliferative lesions of the liver from nodular hyperplasia/dysplasia to adenomas and carcinomas.[40] Females had a very low incidence of liver desease (3%), and hepatocellular carcinoma represented 27% of all liver lesions in this model. Although the frequency of hepatocellular carcinoma was much lower in BKV/*tat* transgenic mice (2.9%), several animals were affected by liver cell dysplasia. This lesion may represent a preneoplastic state. As we observed liver hemangiomas, not only the hepatocytes but also the endothelial cells in the liver seem to be the target of the oncogenic activity.

BKV/*tat* transgenic mice developed B-cell lymphomas significantly more frequently (7.6%) than control animals (2.2%). This oncogenic effect may be due to a cooperation between BKV TAg and *tat*, because transgenic mice for BKV TAg develop lymphoid hyperplasia.[41] Lymphomas in BKV/*tat* transgenic mice differed from those observed in control animals, as they contained a greater number of blastic lymphoid cells and mitotic figures, indicating that cell proliferation was more active in transgenic mice. Conversely, amyloid depositions were common in lymphomas of both groups. Lymphomas and skin adenocarcinomas were observed both in transgenic and in control animals, but with greater frequency and earlier appearance in transgenic than in control mice, suggesting that the transgene may exert an enhancing effect on some oncogenic factor constitutionally active in this strain of mice.

BKV/*tat* transgenic mice developed also numerous hyperplastic/dysplastic and non-neoplastic lesions. Some of them were exclusive, others common to both transgenic and control animals. However, the frequency of the lesions observed in transgenic mice was always significantly higher than in controls. The pathogenic nature of these lesions was distinguished in two types: 1) a proliferative type with evidence of cell hyperplasia (proliferation of fibroblasts and endothelial cells with consequent neoangiogenesis, hyperkeratosis, liver cell dysplasia, and rectal polyps) and sometimes of dysplasia with alteration of normal differentiation (skin ulcers, skin, and liver cysts) and 2) a regressive/degenerative type with inflammation, healing scars, and amyloidosis (eye lesions, phlogosis of the liver and kidneys, and myocardiosclerosis).

The *tat* gene expressed in all cells of transgenic mice may cause modifications of the normal proliferation and differentiation processes as well as of the immune response by activating the expression of cellular genes and by inducing cytokine secretion. Indeed, it was shown that Tat induces the expression of several cytokines, such as tumor necrosis factor,[42] interleukin-2,[43] interleukin-6,[33,44] and transforming growth factor-β.[45] The nature of the cooperation between BKV TAg and Tat protein in the pathogenesis of the lesions appearing in BKV/*tat* transgenic mice seems to be mainly related to the transcriptional activation of *tat* promoter by BKV TAg, which is a potent transactivator of the HIV-1 LTR. As BKV early region was detected in Kaposi's sarcoma,[46] we considered the possibility that BKV TAg participates in the induction of endothelial proliferation in BKV/*tat* transgenic mice. We have established an experimental model by transforming mouse endothelial cells with BKV early region. These transformed endothelial cells, after subcutaneous inoculation into nude mice, did not induce angiogenic tumors. Instead they induced solid tumors with the characteristics of sarcomas, not particularly vascularized. These tumors were surrounded by a thick wall of fibrotic tissue and regressed after a short period of growth. Transformed cells secrete a great amount of transforming growth factor-β, which probably induces the fibrotic process. (A. Corallini et al., manuscript in preparation). Considering these results, it is unlikely that BKV TAg is involved in the endothelial proliferation observed in BKV/*tat* transgenic mice. In addition, transgenic mice for BKV TAg develop a syndrome different from that of BKV/*tat* transgenic mice, characterized by a lymphoproliferative disease and kidney carcinomas.[41] Therefore, with the exception of lymphomas, which may involve a

cooperation between BKV TAg and *tat* in the induction of the pathological phenotype, all of the other pathological features in BKV/*tat* transgenic mice seem to be attributable to *tat* expression.

On the other hand, the transcriptional activation of HIV-1 LTR by BKV TAg seems to be very important in our transgenic mouse model. In fact, BKV/*tat* transgenic mice, where *tat* is expressed in all cells and tissues, developed a variety of pathological phenotypes involving many different organs, whereas mice transgenic only for *tat*, where *tat* expression was detected only in the epidermis and rarely in the liver, developed proliferative skin and liver lesions[35,40] but did not develop other pathological phenotypes.

The appearance of similar lesions in transgenic and in control mice, but with greater frequency, with more severity, and earlier in life in the transgenic group, suggests that *tat* expression is supporting and activating a natural predisposition of these animals to develop such lesions. Finally, many neoplastic and non-neoplastic alterations observed in BKV/*tat* transgenic mice, such as skin tumors, KS-like lesions, lymphomas, liver cell dysplasia, and hepatocarcinomas, and rectum and eye lesions, are similar to the pathological findings observed in AIDS patients, suggesting a relevant role for *tat* in the induction of such lesions during the course of AIDS.

Acknowledgments

We thank A. Bevilacqua, P. Zucchini, M. Bonazzi, and I. Pivanti for excellent technical assistance, C. Lanza and F. Sartore for the histochemical and immunohistochemical reactions, G. Miotti-Scapin and S. Turco for the assistance in ultrastructural observations, and L. Rinaldi and A. Leorin for photographs.

References

1. Beral V, Jaffe H, Weiss R: Cancer, HIV and AIDS. Cancer Surv 1991, 10:1–3
2. Biggar RJ: Cancer in the acquired immunodeficiency syndrome: an epidemiological assessment. Semin Oncol 1990, 17:251–260
3. Cremer KJ, Spring SB, Gruber J: Role of human immunodeficiency virus type 1 and other viruses in malignancies associated with acquired immunodeficiency syndrome. J Natl Cancer Inst 1990, 82:1016–1025
4. Beral V: Epidemiology of Kaposi's sarcoma. Cancer Surv 1991, 10: 5–22
5. Harnly ME, Swan SH, Holly EA, Kelter A, Padian N: Temporal trends in the incidence of non-Hodgkin's lymphoma and selected malignancies in a population with a high incidence of acquired immunodeficiency syndrome (AIDS). Am J Epidemiol 1988, 128:261–267
6. Obrams GI, Grufferman S: Epidemiology of HIV associated non-Hodgkin lymphoma. Cancer Surv 1991, 10:91–102
7. Rabkin C, Blattner WA: HIV infection and cancers other than non-Hodgkin lymphoma and Kaposi's sarcoma. Cancer Surv 1991, 10: 151–160
8. Luxton JC, Thomas JA, Crawford DH: Aetiology and pathogenesis of non-Hodgkin lymphoma in AIDS. Cancer Surv 1991, 10:103–119
9. Giraldo G, Beth E, Kourilsky FM, Henle W, Miké V, Huraux JM, Andersen HK, Gharbi NR, Kyalwazi SK, Puissant A: Antibody patterns to herpes-viruses in Kaposi's sarcoma: serological association of European Kaposi's sarcoma with cytomegalovirus. Int J Cancer 1975, 15:839–848
10. Giraldo G, Beth E, Henle W, Henle G, Miké V, Safai B, Huraux JM, McHardy J, de-Thé G: Antibody patterns to herpes viruses in Kaposi's sarcoma. II. Serological association of American Kaposi's sarcoma with cytomegalovirus. Int J Cancer 1978, 22:126–131
11. Grody WW, Lewin KJ, Naeim F: Detection of cytomegalovirus DNA in classic and epidemic Kaposi's sarcoma by *in situ* hybridization. Hum Pathol 1988, 19:524–528
12. McDougall JK, Olso KA, Smith PP, Collier AC: Detection of cytomegalovirus and AIDS-associated retrovirus in tissues of patients with AIDS, Kaposi's sarcoma and persistent lymphadenopathy. Antibiot Chemother (Mosc) 1987, 38:99–112
13. Rappersberger K, Tschachler E, Zonzits E, Gillitzer R, Hatzakis A, Kaloterakis A, Mann DL, Popow-Kraupp T, Biggar RJ, Berger R, Stratigos J, Wolff K, Stingl G: Endemic Kaposi's sarcoma in human immunodeficiency type 1 seronegative persons: demonstration of retrovirus-like particles in cutaneous lesions. J Invest Dermatol 1990, 95:371–381
14. Huang YQ, Li JJ, Rush MG, Poiesz BJ, Nicolaides A, Jacobson M, Zhang WG, Coutavas E, Abbott MA, Friedman-Kien AE: HPV-16-related DNA sequences in Kaposi's sarcoma. Lancet 1992, 339:515–518
15. Nickoloff BJ, Huang JQ, Li JJ, Friedman-Kien AE: Immunohistochemical detection of papillomavirus antigens in Kaposi's sarcoma. Lancet 1992, 339:548–549
16. Barbanti-Brodano G, Pagnani M, Viadana P, Beth-Giraldo E, Giraldo G, Corallini A: BK virus DNA in Kaposi's sarcoma. Antibiot Chemother (Mosc) 1987, 38:113–120
17. Barbanti-Brodano G, Pagnani M, Balboni PG, Rotola A, Cassai E, Beth-Giraldo E, Giraldo G, Corallini A: Studies on the association of Kaposi's sarcoma with ubiquitous viruses. AIDS and Associated Cancers in Africa. Edited by Giraldo G, Beth-Giraldo E, Clumeck N, Gharbi Md-R, Kyalwazi SK, de Thé G. Basel, S Karger, 1988, pp 175–181
18. Negrini M, Rimessi P, Mantovani C, Sabbioni S, Corallini A, Gerosa A, Barbanti-Brodano G: Characterization of BK virus variants rescued from human tumours and tumour cell lines. J Gen Virol 1990, 71:2731–2736
19. Bovenzi P, Mirandola P, Secchiero P, Strumia R, Cassai E, Di Luca D: Human herpesvirus 6 (variant A) in Kaposi's sarcoma. Lancet 1993, 341:1288–1289
20. Chang Y, Cesarman E, Pessin MS, Lee F, Culpepper J, Knowles DM, Moore PS: Identification of herpesvirus-like DNA sequences in AIDS-associated Kaposi's sarcoma. Science 1994, 266:1865–1869
21. Wong-Staal F, Sadie MR: The Control of Human Retrovirus Gene Expression. Edited by Franza R, Cullen B, Wong-Staal F. Cold Spring Harbor, NY, Cold Spring Harbor Laboratory Press, 1988, pp 1–10
22. Fisher AG, Feinberg MB, Josephs SF, Harper ME, Marselle LM, Reyes G, Gonda MA, Aldovini A, Debouck C, Gallo RC, Wong-Staal F: The trans-activator gene of HTLV-III is essential for virus replication. Nature 1986, 320:367–371
23. Ensoli B, Barillari G, Salahuddin SZ, Gallo RC, Wong-Staal F: Tat protein of HIV-1 stimulates growth of cells derived from Kaposi's sarcoma lesions of AIDS patients. Nature 1990, 345:84–86
24. Ensoli B, Buonaguro L, Barillari G, Fiorelli V, Gendelman R, Morgan RA, Wingfield P, Gallo RC: Release, uptake, and effects of extracellular human immunodeficiency virus type 1 Tat protein on cell growth and viral transactivation. J Virol 1993, 67:277–287
25. Frankel AD, Pabo CO: Cellular uptake of the Tat protein from human immunodeficiency virus. Cell 1988, 55:1189–1193
26. Helland DE, Welles JL, Caputo A, Haseltine WA: Transcellular transactivation by the human immunodeficiency virus type 1 Tat protein. J Virol 1991, 65:4547–4549
27. Barillari G, Gendelman R, Gallo RC, Ensoli B: The tat protein of human immunodeficiency virus type 1, a growth factor for AIDS Kaposi's sarcoma and cytokine-activated vascular cells, induces adhesion of the same cell types by using integrin receptors recognizing the RGD amino acid sequence. Proc Natl Acad Sci USA 1993, 90:7941–7945
28. Albini A, Fontanini G, Masiello L, Tacchetti C, Bigini D, Luzzi P, Noonan DM, Stetler-Stevenson WG: Angiogenic potential *in vivo* by Kaposi's sarcoma cell-free supernatants and HIV-1 *tat* product: inhibition of KS-like lesions by tissue inhibitor of metalloproteinase-2. AIDS 1994, 8:1237–1244
29. Albini A, Barillari G, Benelli R, Gallo RC, Ensoli B: Tat, the human immunodeficiency virus type 1 regulatory protein, has angiogenic properties. Proc Natl Acad Sci USA 1995, 92:4838–4842
30. Albini A, Benelli R, Presta M, Rusnati M, Ziche M, Rubartelli A, Paglialunga G, Bussolino F, Noonan D: HIV-tat protein is a heparin-binding angiogenic growth factor. Oncogene 1996, 12:289–297

31. Vaishnav YN, Wong-Staal F: The biochemistry of AIDS. Annu Rev Biochem 1991, 60:577–630
32. Buonaguro L, Barillari G, Chang HK, Bohan CA, Kao V, Morgan R, Gallo RC, Ensoli B: Effects of the human immunodeficiency virus type 1 Tat protein on the expression of inflammatory cytokines. J Virol 1992, 66:7159–7167
33. Scala G, Ruocco MR, Ambrosino C, Mallardo M, Giordano V, Baldassarre F, Dragonetti E, Quinto I, Venuta S: The expression of interleukin 6 gene is induced by the human immunodeficiency virus type 1 Tat protein. J Exp Med 1994, 179:961–971
34. Ensoli B, Gendelman R, Markham P, Fiorelli V, Colombini S, Raffeld M, Cafaro A, Chang HK, Brady J, Gallo RC: Synergy between basic fibroblast growth factor and HIV-1 Tat protein in induction of Kaposi's sarcoma. Nature 1994, 371:674–680
35. Vogel J, Hinrichs SH, Reynolds RK, Luciw PA, Jay G: The HIV *tat* gene induces dermal lesions resembling Kaposi's sarcoma in transgenic mice. Nature 1988, 355:606–611
36. Corallini A, Altavilla G, Pozzi L, Bignozzi F, Negrini M, Rimessi P, Gualandi F, Barbanti-Brodano G: Systemic expression of HIV-1 *tat* gene in transgenic mice induces endothelial proliferation and tumors of different histotypes. Cancer Res 1993, 53:5569–5575
37. Bancroft JD, Stevens A: Theory and Practice of Histological Techniques. Edinburgh, Churchill Livingstone, 1982
38. Pattengale PK: Tumours of the lymphohaematopoietic system. World Health Organization Pathology of Tumours in Laboratory Animals, vol 2: Tumors of the Mouse, ed 2. Edited by Turusov VS, Mohr U. IARC, Lyon, 1994, pp 651–670
39. Sambrook J, Fritsch EF, Maniatis T: Molecular Cloning: A Laboratory Manual, ed 2. Cold Spring Harbor, NY, Cold Spring Harbor Laboratory Press, 1989
40. Vogel J, Hinrichs SH, Napolitano LA, Ngo L, Jay G: Liver cancer in transgenic mice carrying the human immunodeficiency virus *tat* gene. Cancer Res 1991, 51:6686–6690
41. Dalrymple SA, Beemon KL: BK virus T antigen induces kidney carcinomas and thymoproliferative disorders in transgenic mice. J Virol 1990, 64:1182–1191
42. Buonaguro L, Buonaguro FM, Giraldo G, Ensoli B: The human immunodeficiency virus type 1 Tat protein transactivates tumor necrosis factor beta gene expression through a TAR-like structure. J Virol 1994, 68:2667–2682
43. Westendorp MO, Li-Weber M, Frank RW, Krammer PH: Human immunodeficiency virus type 1 Tat upregulates interleukin-2 secretion in activated T cells. J Virol 1994, 68:4177–4185
44. Rautonen J, Rautonen N, Martin NL, Wara DW: HIV type 1 Tat protein induces immunoglobulin and interleukin 6 synthesis by uninfected peripheral blood mononuclear cells. AIDS Res Hum Retroviruses 1994, 10:781–785
45. Zauli G, Davis BR, Re BR, Visani MC, Furlini G, La Placa M: Tat protein stimulates production of transforming growth factor-beta 1 by marrow macrophages: a potential mechanism for HIV-1 induced hematopoietic suppression. Blood 1992, 80:3036–3043
46. Monini P, Rotola A, de Lellis L, Corallini A, Secchiero P, Albini A, Benelli R, Parravicini C, Barbanti-Brodano G, Cassai E: Latent BK virus infection and Kaposi's sarcoma pathogenesis. Int J Cancer 1996, 66:717–722